Volume 64, Issue 2, 2020
Journal of Scientific Research
Institute of Science,
Banaras Hindu University, Varanasi, India.

Petrographic and Microthermometric Measurment of Fluid Inclusions and its Constraints on Genesis of the Paleoproterozoic Carbonate-hosted Pb-Zn Deposit at Rajpura-Dariba, Rajasthan, India: Possibility of Fluid-mixing

Juned Alam*, and F. N. Siddiquie
Department of Geology, A.M.U. Aligarh, India.
juned.iit87@gmail.com*

Abstract: **The Dariba Zn-Pb mineralizations are situated in the southern part of Rajpura-Dariba Bethumni Belt, Rajasthan, India. This study includes the fluid inclusions petrography and microthermometry in quartz samples, associated commonly with calc-silicate bearing dolostone and graphite-mica-schist. The different salinities and homogenization temperatures values were determined in the primary fluid inclusions in quartz. The microthermometric data indicate that four major types of fluids were responsible for the formation of the ore deposits. They are Type-I aqueous biphase inclusions, Type-II monophase CO_2 inclusions, Type-III biphase aqueous-carbonic inclusions and Type-IV polyphase aqueous-carbonic inclusions. The Type-I and Type-III inclusions are more abundant than other inclusions. The observed and calculated data like the first and last ice melting temperature is an indicator of presence of salt in inclusions. The salinity of Type-I inclusions ranges from 4.15 to 13.26 wt% NaCl equivalent and temperature of total homogenization (Th) values are in the range of 98.2° to 135°C, with most values between 102° and 122°C while the salinity of Type-III inclusions ranges from 3.95 to 13.26 wt% NaCl equivalent and the temperature of total homogenization ranges from 250 to 290°C at pressure of 1.2 to 2 kbar, corresponding to a depth of mineralization at 0 - 1.8 kms. The density of aqueous-carbonic inclusions measured in quartz samples varied from 0.65 to 0.96 g/cm^3. Low salinity and low to medium temperature of homogenization of inclusions reveals that the cooling is the important mechanism for the mineralization of ore deposits, according to inclusion, i.e. composition, vapour and liquid may be the main agents for transport of Pb and Zn.**

Index Terms: **Fluid inclusion, Microtherometry, Pb-Zn mineralization, Petrography, Rajpura-Dariba, Rajasthan**

I. INTRODUCTION

Fluid inclusions have been used extensively to characterize the nature of crustal fluids and in particular, the composition of hydrothermal fluids is responsible for various types of mineral deposits. The Pb-Zn mineralization in the Rajpura-Dariba bethumni belt is mostly stratiform, associated commonly with calc-silicate bearing dolostones, carbonaceous chert and graphite-mica-schict. CH_4, CO_2 and N_2 have been reported by various workers from other carbonate-hosted Pb-Zn deposits (Haynes et al., 1989; Jones and Kesler 1992; Conliffe et al., 2013; Huizenga et al., 2006 and Kesler et al., 2007).

The salinity of fluids responsible for massive type ore at Dariba is generally between 5 to 10 wt% NaCl equivalent with a total observed range of 3.95 to 13.26 wt% NaCl equivalent (Table 2). The total range of salinity in VMS fluid inclusion is between 0 and 30 wt% NaCl equivalent (or NaCl+$CaCl_2$), indicating seawater modification either by water-rock interaction, or by phase separation, or by addition of magmatic fluid, or by some combination of these processes (Bodnar et.al., 2014). The ore deposits of Rajpura-Dariba are well known for their prominent Pb-Zn sulfide mineralization hosted by Proterozoic carbonate rocks of the Aravalli Supergroup, which are located 76 kms south of District Udaipur, Rajasthan, India. The current study is focused on SK mine where the samples of quartz are associated with vein and massive type galena and

* Corresponding Author

sphalerite ores. An attempt has been made to describe the various types of fluid inclusions associated with the Rajpura-Dariba Pb-Zn mineralization along with the results of microthermometric data. This data will provide the salinities and densities of the inclusions to determine the P-T conditions of mineralization and the origin of the ore bearing fluids as well.

II. Geological Setting

The geology of Rajasthan has been studied by many experts over decades and the different major geological units and prominent faults and lineaments of this region were reported. The Aravalli sequence was recognized by Heron (1953) to be the oldest cover sequence laid down over the pre-Aravalli rocks, consisting of the Banded Gneissic Complex and the Bundelkhand Gneiss (Berach Granite), with a pronounced unconformity at the base of the cover sequence. Structural and metamorphic studies of the pre-Aravalli rocks indicate that these metasedimentary and meta-igneous rocks were deformed and metamorphosed prior to the deposition of the oldest cover sequence (Heron, 1953; Roy and Das, 1985; Roy, 1988; Sharma et. al., 1988 and Sharma & Rahman, 1995). The cratonization of this segment of the crust is believed to have been achieved by 2500 Ma (Roy, 1988), although the Archean pre-Aravalli metamorphic event was much earlier (Sharma and Rahman, 1995).

Rajpura- Dariba area ($24^0$57': $74^0$08', 45 L/1) located at the southern extremity of the belt (Fig. 1**)**. This belt is located at a distance of 76 Km, from Udaipur City. The cover rocks extend over 19 km in north-south direction as crescent-shaped regional synform with closure towards south of Dariba. Gupta (1934) first recorded the old workings and ferrugineous breccia in Rajpura-Dariba area and put them in Aravalli Group. Gupta et. al., (1980) classified the supracrustal metasedimentry and metavolcanic rocks of this 20 kms long belt of Rajpura-Dariba Group, a part of Bhilwara Super Group, and finally put them in Bhilwara tectonic belt. The Rajpura-Dariba Group lies unconformably over the gneisses and migmatites of the Mangalwar Complex (BGC of Heron, 1953). Poddar and Chatterjee (1965), Basu (1966) and Raja Rao (1967) classified the rocks of Dariba-Surawas area as Rajpura-Dariba Group and Mangalwar complex. Samaddar and Das Gupta (1990) divided the rocks of the Dariba-Bethumni belt into six different lithounits as: Inner calcareous mica schist, Inner carbonaceous schist with staurolite and kyanite, Outer interbanded mica schist with metachert, Outer carbonaceous schist (± staurolite and kyanite), Dolomite marble, Mica schist with porphyroblasts of garnet, staurolite & kyanite and Migmatites, gneiss and banded gneissic complex. Yadav and Sharma (1991) have modified the lithologcal succession given by Samaddar (1990) on the basis of lithology observed in the boreholes and regional traverse taken by them in the area.

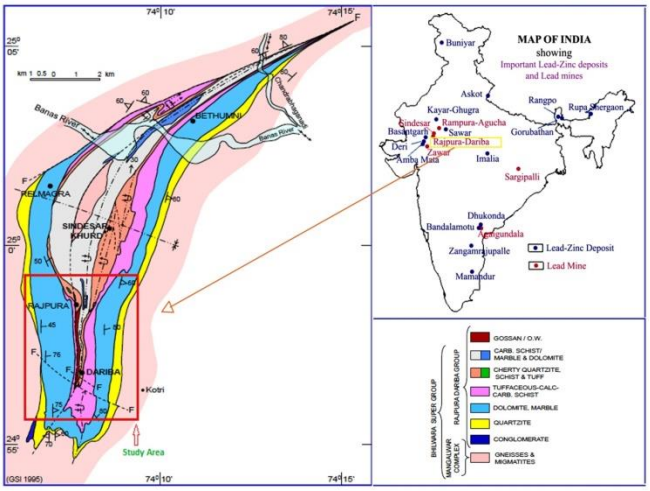

Fig. 1. Geological Map of Rajpura-Dariba-Bethumni-Surawas Belt. Records of GSI Volume 129 (7), 1995.

III. Materials and Methodology

The study of 60 wafer and doubly polished thin section for petrographic features of fluid inclusions in the different types of quartz veins samples taken from: Unmineralized quartz vein samples from surface exposures, Quartz associated with vein-type ore, Quartz associated with massive galena and sphalerite ore. The doubly polished wafers thin sections need to be prepared with the general method outlined by Shepherd et al (1985). Gangue quartz, which gave doubtful relationship with the ores, was avoided for present study.

The micro thermometric analysis were carry out by using a Chaixmeca stage (-196 to +600^0C) fitted on a Leitz Laborlux microscope at the Department of Earth Sciences, Indian Institute of Technology, Roorkee (U.K.). The accuracy of temperature measurement is about $\pm$ 0.5^0C. The purpose of micro thermometric analysis is to observe the different phase transitions within the fluid inclusions in response to temperature changes.

IV. Results

A. Fluid inclusions Petrography

Petrographic observations, field relations and fluid inclusions data were used to characterize the mineralizing fluids of lead-zinc bearing quartz veins, which are spatially associated with Micaceous schist, Calc-silicate and Dolomite in the Dariba area. Fluid inclusions in quartz samples from the study area can be classified as primary, secondary or pseudo-secondary, respectively (e.g. Roedder, 1984 and Van den Kerkhof & Hein, 2001). The inclusions in clusters and isolated inclusions were considered as primary with respect to the formation of quartz vein. Only the primary inclusions (5–24 μm) were studied in detail. The nature of fluid inclusions is discussed below.

1) *Type I (Aqueous Biphase)*

The type I inclusions are 5 to 20 µm in size and primary in origin which occur as an isolated inclusion. Two phases are present at room temperature in this type of inclusions which are mainly liquid and gas with predominance of liquid (Fig. 2). The liquid and gas content vary from liquid 75 - 90 percent and gas content in the range of 10 - 25 percent. These inclusions are equant, subhedral and subrounded to irregular in shape. These type of inclusions are associated with the sulphide stage of mineralization.

Fig. 2. Photomicrograph of quartz showing aqueous Biphase subrounded isolated Fluid Inclusion at room temperature. SK mine of Rajpura-Dariba-Bethumni Belt, Rajasthan.

2) *Type II (monophase CO_2)*

Type II inclusions are monophase inclusions at room temperature. These inclusions vary in size from 5 to 22 µm. Some inclusions are subrounded to subhedral in shape, but many of them observed are irregular in shape (Fig. 3). The distribution of this type of fluid inclusions are uniform throughout the samples and no preferred orientation is observed. On the basis of their spatial distribution these inclusions are inferred to be primary in origin. A vapour bubble developes during cooling. Compositionally these are apparently pure CO_2.

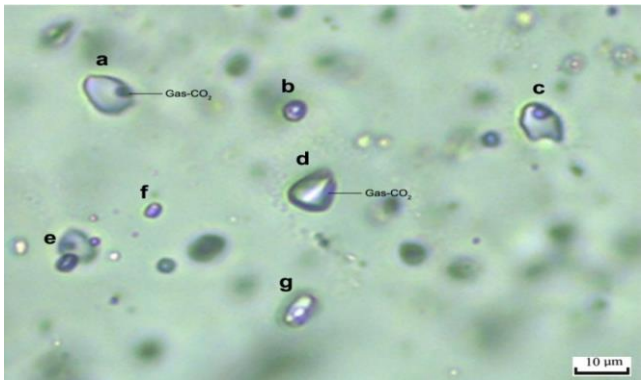

Fig. 3. Photomicrographs of quartz showing CO_2 rich monophase dark subrounded isolated Fluid Inclusiosn at room temperature. SK mine of Rajpura-Dariba-Bethumni Belt, Rajasthan.

3) *Type III (biphase aqueous-carbonic inclusions)*

Type III inclusions are biphase aqueous-carbonic inclusions consist of two phases with a bubble in aqueous phase at room temperature, but during freezing a new phase appears exhibiting liquid H_2O, liquid CO_2 and vapour CO_2. This inclusion ranges in size from 4 to 24 µm having different shapes such as rounded, sub-rounded and irregular (Fig. 4).

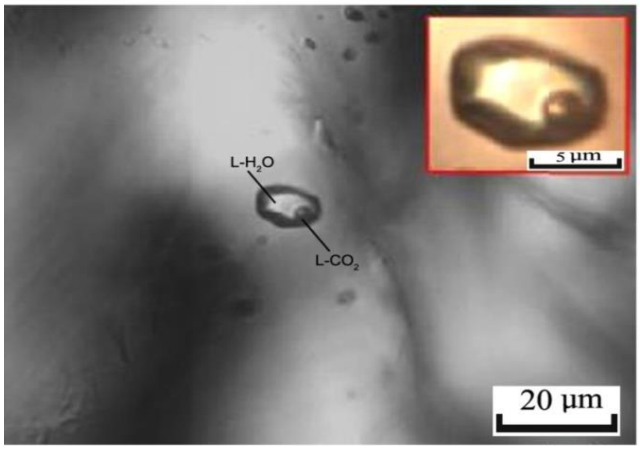

Fig. 4. Photomicrograph of quartz showing aqueous-carbonic sub-rounded shape isolated Fluid Inclusions at room temperature. SK mine of Rajpura-Dariba-Bethumni Belt, Rajasthan.

4) *Type IV (Polyphase aqueous-carbonic inclusions)*

Type IV inclusions are polyphase aqueous-carbonic inclusions consist of three phases, showing bubble inside a bubble with aqueous phase at room temperature (Fig. 5). These inclusions were formed by trapping of a homogeneous H_2O-CO_2 mixture which characteristically show two immiscible liquids at room temperature, a CO_2 rich phase and a H_2O phase, additionally there is a CO_2 rich vapour bubble within the liquid CO_2.

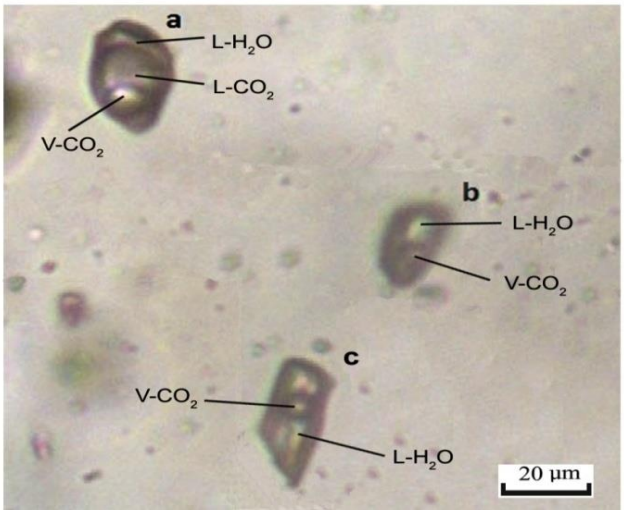

Fig. 5. Photomicrograph of quartz showing aqueous-carbonic polyphase Fluid Inclusions having liquid-H_2O, liquid-CO_2 and gaseous CO_2 at room temperature. SK mine of Rajpura-Dariba-Bethumni Belt, Rajasthan

B. Microthermometry Analysis

Microthermometric runs were taken on primary inclusions in the collected Quartz samples associated with the mineralization. Only those inclusions, which do not show any evidence of leakage or necking down and occur away from the healed cracks, were chosen for present peace of research work.

Type I: Type I are the biphase aqueous inclusion where liquid is the dominant phase. The homogenization temperature recorded by the disappearance of the tiny bubble. The inclusions have values of T_mIce in the range of –7.2° to –2.3°C (Table I**)** and corresponding salinities of 4.15 to 13.26 wt% NaCl equivalent. Homogenization is always into the liquid state by vapour disappearance (L+V →L) and Th values are in the range of 98.2° to 135°C, with most of the values between 102° and 122°C.

Type II: Type II inclusions are monophase inclusions show complete solid CO_2 melting ($T_m(CO_2)$) between –56.4°C to –57.4°C (Table II), indicating that these inclusions consist of CO_2 with minor amount of other gases like N_2 and CH_4. These inclusions homogenize to a single phase below room temperature during heating runs. Temperature of homogenization of CO_2 (Th(CO_2)) varies from +10.6° to +29.3°C (Table II). Homogenization is always into liquid state by vapour disappearance. Although these inclusions are apparently monophase CO_2 inclusions.

*Type III***:** Type III are biphase aqueous-carbonic inclusions at room temperature having two phases with a bubble in aqueous phase. Upon cooling this type of inclusions developed a vapour bubble in the CO_2 rich phase between -6ºC to -17ºC. At around -28ºC to -33ºC first freezing takes place with a change in the shape of the CO_2 liquid phase. A solid with a radial texture is formed between the boundary of CO_2 and H_2O **(**Fig. 4) rich phase of the inclusions. Upon gradual heating from –100°C, the solid CO_2 completely melts at just below the triple point of CO_2 (–56.6°C), giving rise to liquid CO_2 and vapour and indicating that the nonaqueous gaseous phase is almost pure CO_2. The assemblage of ice, liquid CO_2, clathrate, and vapour observed in inclusions may be a disequilibrium assemblage, resulting from the barrier formed by clathrate between the liquid, aqueous, and carbonic phases, as suggested by Diamond (1994). Ice melting proceeds in inclusions up to –2.5°C, although final ice melting is not observable in majority of thr cases because of the presence of clathrate. The final melting of clathrate is observed between +2 to +8°C (Table III**)**.

The homogenization of CO_2 in most inclusions is into the liquid phase by vapour disappearance ($LCO_2 + V \rightarrow LCO_2$). Only in a few inclusions the homogenization of CO_2 phases into vapour phase ($LCO_2 + V \rightarrow V$) was observed. The homogenization temperatures of CO_2 phases (Th(CO_2)) vary widely, with values ranging between +10.5° to +29.6°C (Table III). Temperature of total homogenization (Th(total)) also varies widely. In all the cases where measurements were possible, values of Th(total) was observed between 250°C to 290°C.

Type IV: The inclusions of type IV are also aqueous-carbonic inclusions but polyphase at room temperature having three phase-aqueous liquid, CO_2 Liquid and CO_2 vapour (Fig. 5**)**. Type IV inclusions do not develop another vapour bubble like III inclusions while cooling. During the cooling, sudden collapse of the CO_2 phase and complete solid ice formation is observed between –50° and –52°C. Further cooling up to –100°C does not have any effect on the inclusions. While reheating, there is no change in these inclusions around –56.6°C, which is triple point of CO_2. In some larger inclusions of 15 to 25 μm size, repeated cycling between 10° and 5°C results in a radial growth of clathrate from the CO_2 phase. These grains melt between 6° and 8°C (Table III), indicating that it is clathrate. In smaller (5–8 μm size) inclusions clathrate formation could not be observed. The total homogenization (Th(total)) in these inclusions are always via bubble-point transition and ranges from 240° C to 290°C.

Table I. Microthermometry data of aqueous fluid inclusion (Type I).

S.No.	L : V at room temperature	T_hTOT (°C)	T_{FM}Ice (°C)	T_m Ice (°C)	Salinity Wt % NaCl eq.
1.	60 : 40	+100 (L)	-15	-7.2	13.26
2.	70 : 30	+95(L)	-20	-3.7	6.67
3.	50 : 50	+99(L)	-19	-3.2	5.76
4.	40 : 60	+110(L)	-25	-3.3	5.97
5.	60 : 40	+112(L)	-18	-3.3	5.97
6.	50 : 50	+120(L)	-29	-3.4	6.15
7.	30 : 70	+105(L)	-17	-2.4	4.30
8.	70 : 30	+130(L)	-30	-2.5	4.47
9.	45 : 55	+104(L)	-27	-2.5	4.47
10.	50 : 50	+98.2(L)	-23	-2.4	4.30
11.	65 : 35	+135(L)	-19	-5	7.86
12.	60 : 40	+130(L)	-22	-7.2	13.26
13.	80 : 20	+110(L)	-30	-6	9.20
14.	90 : 10	+105(L)	-21	-7.2	13.26
15.	25 : 75	+125(L)	-30	-3.5	6.35
16.	60 : 40	+130(L)	-20	-4.5	7.15
17.	80 : 20	+130(L)	-22	-5.5	8.54
18.	15 : 85	+125(L)	-29	-3.6	6.55
19.	50 : 50	+120(L)	-26	-3.4	6.15

Table II. Microthermometry data of carbonic fluid inclusion (Type II)

S.N.	T_m CO_2 (°C)	T_h CO_2 (°C)
1.	-56.5	+12.3(L)
2.	-56.6	+15.1(L)
3.	-56.8	+20.8(L)
4.	-56.3	+15.2(L)
5.	-56.7	+14.9(L)
6.	-57.0	+19.1(L)
7.	-56.9	+26.7(L)
8.	-56.8	+20.4(L)
9.	-56.9	+18.8(L)
10.	-56.6	+29.3(L)
11.	-56.5	+11.2(L)
12.	-57.0	+10.6(L)
13.	-56.2	+18.5(L)
14.	-56.6	+14.3(L)
15.	-56.7	+19.7(L)

Table III. Microthermometry data of aqueous-carbonic fluid inclusion (Type III).

S.No.	$H_2O : CO_2$ At room temperature	T_m of CO_2(°C)	T_h of CO_2 (°C)	T_h of TOT (°C)	T_{FM} of Ice (°C)	T_m of CL (°C)	Salinity Wt % NaCl eq.	Density
1	70:30	-56.6	+20.1(L)	265(L)	-23	+4	10.58	0.8594
2	50:50	-56.7	+25.3(L)	255(L)	-20	+6	7.47	0.8213
3	70:30	-56.5	+26.4(L)	270(L)	-19	+3	11.97	0.7564
5	60:40	-56.5	+15.6(L)	260(L)	-21	+4.5	9.84	0.8045
6	30:70	-56.2	+16.8(L)	275(L)	*	+3.4	11.43	0.6967
7	30:70	-56.3	+25.3(L)	255(L)	*	+8	3.95	0.7081
8	50:50	-56.9	+26.4(L)	275(V)	-27	+6	7.47	0.7566
9	60:40	-56.5	+25.4(L)	280(L)	-19	+5.4	8.45	0.8945
10	40:60	-56.6	+15.6(L)	285(L)	-18	+4	10.58	0.7087
1	60:40	-56.6	+24.5(L)	280(L)	-23	+8	3.95	0.8867
12	80:20	-56.1	+15.6(L)	260(V)	-20.5	+6	7.47	0.8125
13	50:50	-56.0	+17.6(L)	290(L)	-21.3	*	*	0.6567
14	80:20	-56.8	+10.5(L)	285(L)	*	+6	7.47	0.7767
15	70:30	-55.9	+12.3(L)	265(L)	-17	+2.5	12.63	0.8750
16	70:30	-57.1	+14.5(L)	250(L)	-26	+3.5	11.29	0.6871
17	10:90	-57.2	+15.1(L)	190(L)	-26	+5.7	7.97	0.7845
18	10:90	-55.9	+23.4(L)	200(V)	-21	+7	5.77	0.8455
19	50:50	-56.6	+21.5(L)	260(L)	*	*	*	0.8095
20	50:50	-57.2	+25.6(L)	255(L)	-19	+7	5.77	0.8095
21	60:40	-56.2	+10.5(L)	290(L)	-18	+3	11.97	0.7545
22	60:40	-56.6	+28.5(L)	285(V)	-21	+3.5	11.29	0.7085
23	50:50	-55.9	+14.2(L)	255(L)	-24	+6.5	6.64	0.6845
24	70:30	-56.5	+25.4(L)	260(L)	-21	+4.4	9.99	0.9145
25	80:20	-56.5	+21.5(L)	270(L)	*	+5.5	8.29	0.9245
26	90:10	-56.6	+10.5(L)	220(V)	-25	+6	7.47	0.8790
27	60:40	-55.8	+30.1(L)	230(V)	-18.5	+2.5	12.63	0.7988
28	30:70	-56.7	+13.5(L)	270(L)	*	+4.5	9.84	0.8545
29	30:70	-57.0	+29.6(L)	250(L)	-19	+4	10.58	0.7045
30	50:50	-56.0	+14.25(L)	200(V)	-20	+5	9.08	0.6945
31	20:80	-56.5	+15.5(L)	220(L)	-28	+5.5	8.29	0.7755
32	60:40	-56.4	+25.6(L)	250(L)	-25	+2	13.26	0.7566
33	60:40	-56.3	+24.5(L)	240(L)	-22	+8	3.95	0.7755
34	80:20	-56.7	+24.9(L)	250(L)	-22	+8	3.95	0.6785
35	60:40	-56.5	+19.6(L)	250(L)	-20.5	+7	5.77	0.6945
36	50:50	-56.6	+26.4(L)	270(L)	-21	*	*	0.7890
37	30:70	-56.6	+28.3(L)	265(L)	-24	+5.5	8.29	0.8975
38	70:30	-56.9	+26.4(L)	275(V)	-21	+7.5	4.87	0.9045
39	50:50	-56.8	+15.5(L)	280(L)	-18	+8	3.95	0.8765
40	70:30	-57.0	+18.5(L)	230(L)	-19	*	*	0.7745

(L) - Liquid state Homogenization
(V) - Vapour state Homogenization
T_h TOT - Total Homogenization temperature
T_h CO_2 - Total Homogenization temperature of CO_2
T_m CO_2 - First melting of CO_2 temperature
T_m CL - Temperature of clathrate melting
T_{FM} Ice - First melting of Ice temparature
T_m Ice - Final melting of Ice temparature
*- - Not observed

V. Phase Observation during Microthermometry (Freezing and Heating Run)

During the freezing and heating run fluid inclusions show variation in colour, size and phases on different temperature (Figs. 6 & 7). During the freezing run, we can calculate the composition of fluid inclusion by observing of first melting of ice (T_{FM} Ice). The estimation of salinity of fluid inclusion can be measure by observing the final melting of ice (Tm Ice). During the heating run, the temperature of homogenization can be calculated.

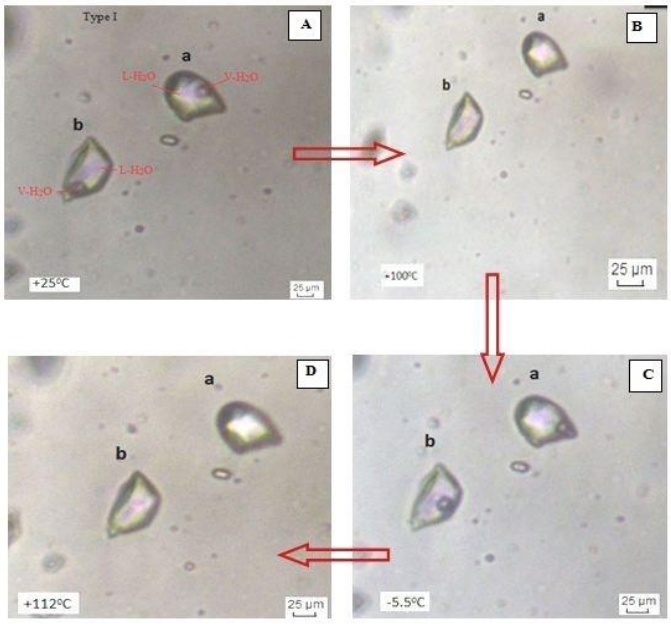

Fig. 6. Phase changes observation of aqueous fluid inclusion (type I) during heating-freezing stage.

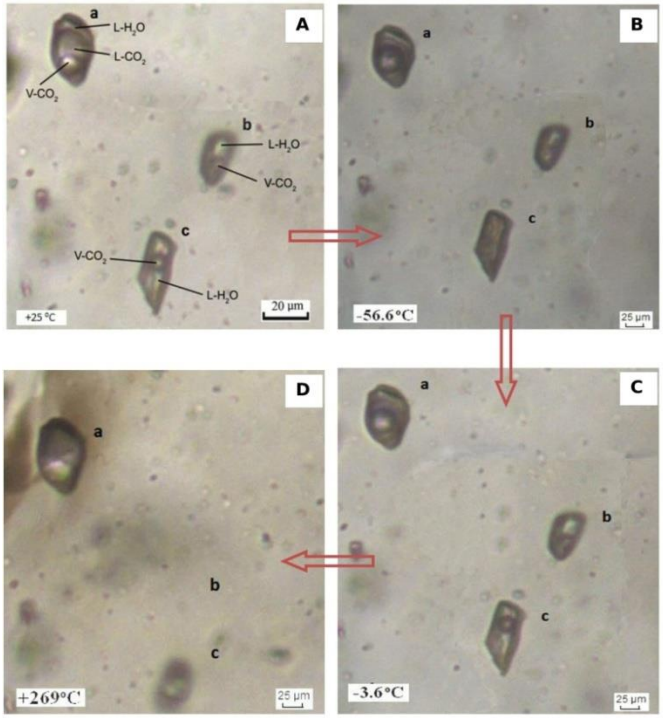

Fig. 7. Phase changes observation of aqueous-carbonic fluid inclusion (type III) during heating-freezing stage.

VI. Estimation of P-T Conditions of Fluid Entrapment

The isochores obtained from the H_2O and CO_2 phases show a pressure of trapping of around 1.2 - 2 kbar and a temperature up to 350°C (Fig. 8). The estimation of P-T condition of fluid inclusions were carefully selected. Carbonic and aqueous phases of inclusions showing maximum peaks from the systems of H_2O-NaCl, H_2O-CO_2-NaCl and also pure carbonic inclusions were selected. The intersection of the isochors of these inclusions are taken as the P-T estimates of the Rajpura-Dariba-Bethumni mineralization. If the fluid inclusions show the accumulation of homogeneously trapped inclusions, then it is clear that the original P-T conditions of entrapment cannot be measure from fluid inclusions evidence alone. The T_hTOT (estimated by microthermometry) and the pressure of homogenization (obtained from a quantitative phase diagram) define only as minimum constraints on the entrapment conditions. The isochores thus produced also yields the ratio of the entrapment P-T conditions, but an independent fluid barometer (pressure correction) or thermometer is required to determine the exact conditions by intersection with the isochors (Diamond 2001).

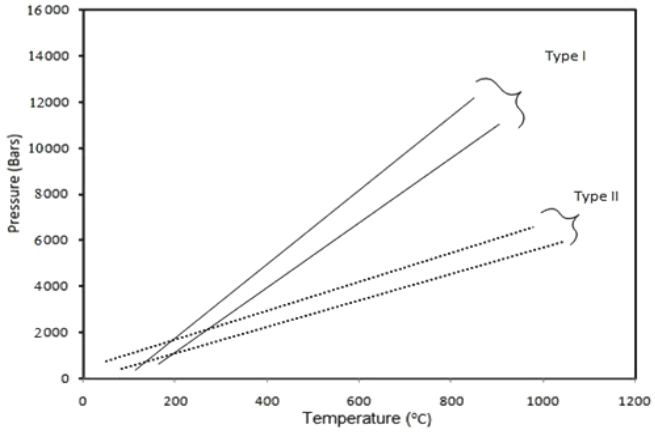

Fig. 8. Isochores for Type I and Type II inclusions to estimate P-T condition of fluid inclusions of Rajpura-Dariba-Bethumni mineralization from the Aqueous and Carbonic inclusions, in each case the end members of homogenization temperatures are taken.

VII. Evolution of Fluid

Fluid inclusions in quartz, associated with sulphide ore mineralization show a wide variety of inclusion types, ranging from apparently pure CO_2 to H_2O-CO_2-NaCl and H_2O-NaCl fluids. Fluid inclusion petrography shows that type I, II, and III inclusions are primary inclusions and that no post-entrapment modifications such as necking or leaking are present. The characteristics of type IV inclusions indicate the possibility of modified inclusions and therefore they are not taken into consideration regarding the properties of the parent primary fluids. The observed and calculated data like the first ice melting temperature (also known as the eutectic melting Te), the composition of the trapped fluid can be deduced. The micro-

thermometric results suggest the presence of aqueous fluid represented by Type I fluid inclusions. The first melting temperature of ice in the inclusions is quite variable in the range of -15°C to -30°C. The aqueous inclusions having final melting temperatures of ice (T_m) below 0.0^0C, is an indicator of presence of salt in inclusions. The frequency of last melting of ice temperature range from -7.2°C to -2.4°C suggests the saline nature of inclusions (Alam, 2019). The higher final melting temperature of ice suggests low internal pressure (e.g. Goldstein and Reynolds, 1994). The frequency curve to determined densities of the fluid ranges between 0.65 to .92 g/ cc (after Archer, 1992) which indicate comparatively low fluid density. Histograms (Fig. 9) showing the different microthermometric parameter of different fluid inclusion, which are suggesting the hydrothermal nature of the fluid during heating of these inclusions. It is, therefore suggested that the hydrothermal fluid responsible for the sulphide mineralization in the study area. Such fluids have also been reported from the other deposits of world (Morrow, 1998; Aulstead et al., 1988; Coniglio et al., 1994 and Nelson et al., 2002).

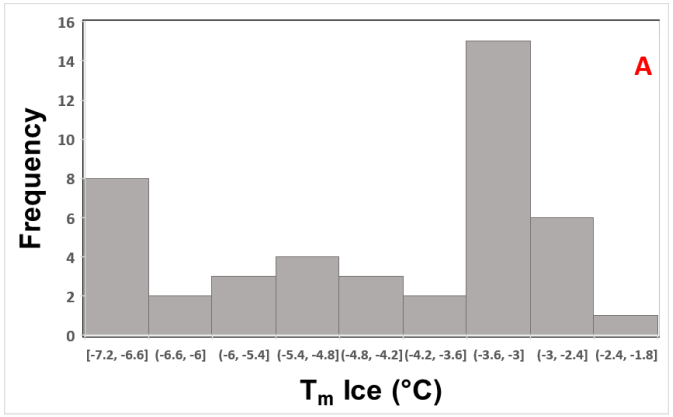

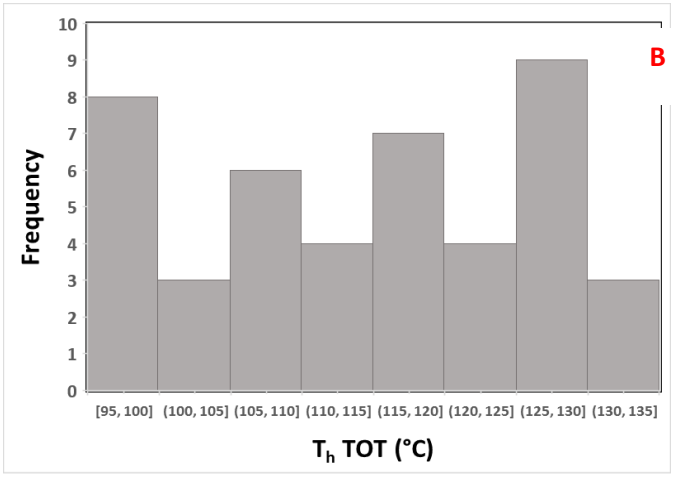

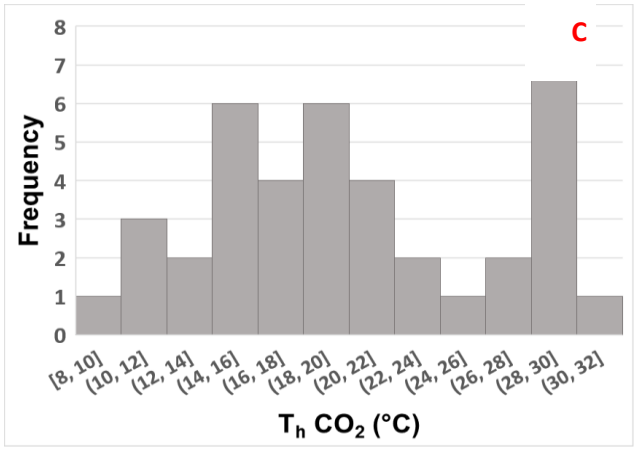

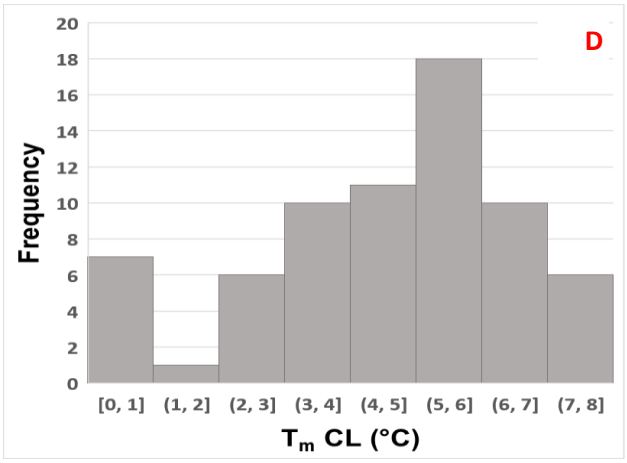

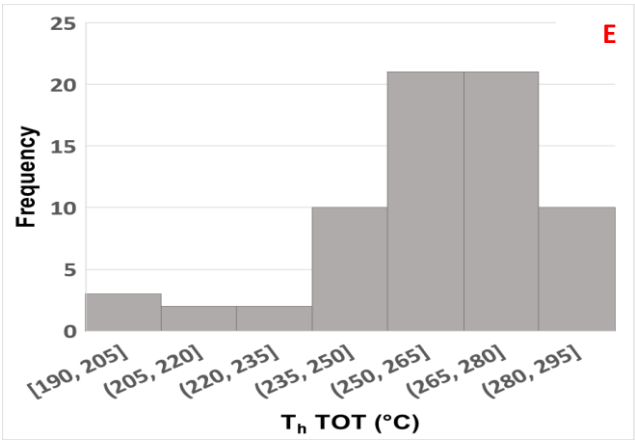

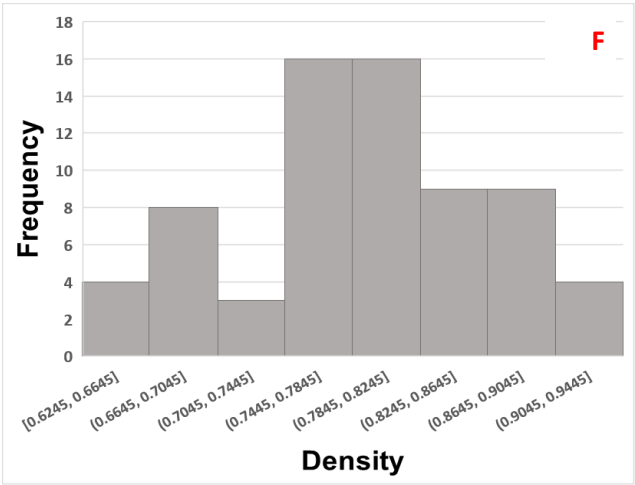

Fig. 9. Histograms showing
(A) T_m Ice v/s frequency of aqueous fluid inclusion (Type I).
(B) Temperature of homogenization v/s frequency of aqueous fluid inclusion (Type I).
(C) T_hCO_2 v/s frequency of carbonic fluid inclusion (Type II).
(D) T_mCL v/s frequency of aqueous-carbonic fluid inclusion (Type III).
(E) T_h TOTv/s frequency of aqueous-carbonic fluid inclusion (Type III).
(F) Density v/s frequency of aqueous-carbonic fluid inclusion (Type III).

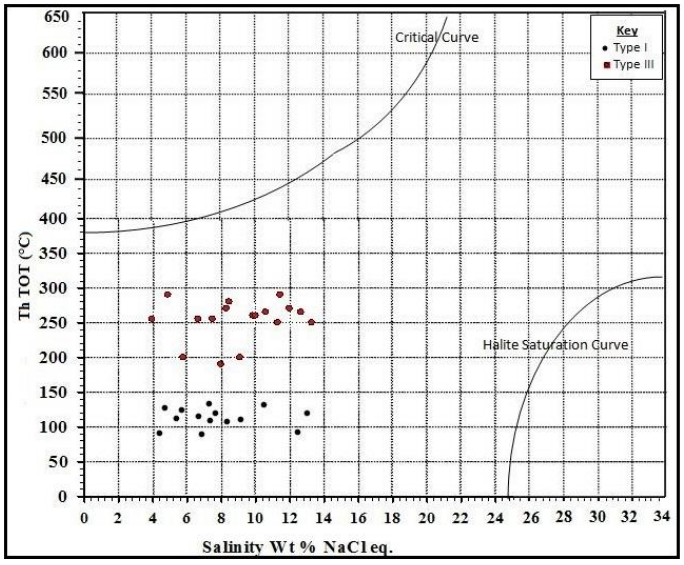

Fig. 10. Plot showing Th TOT v/s salinity of type I & type III inclusions.

VIII. Discussion

Homogenization temperatures of type I inclusions ranges from 98.2° C to 135°C, with most values between 102°C and 122°C (Table I). After being frozen, the first liquid was observed at -30 °C to -15ºC and the temperatures of final ice melting were -7°C to -3.2°C. Salinities were calculated from the final melting temperature of ice using the equation of Bodnar (1993) the salinities are ranging from 4.15 to 13.26 Wt % NaCl eq. with an average 8.5 Wt% NaCl eq. The salinity data correlated with the similar works done by Wilkinson, (2001), Tun et al., (2014) show good correlation. Type II inclusions are monophase inclusions so phase transition was difficult to observe because of their dark appearance. However, there are some inclusions in which phase changes were identified by careful observation. These inclusions show complete solid CO_2 melting ($Tm(CO_2)$) between –56.4°C to –57.4°C (Table II), indicating that these inclusions consist of CO_2 with minor amount of other gases like N_2 and CH_4. These inclusions homogenize to a single phase below room temperature during heating runs. Temperature of homogenization of CO_2 ($Th(CO_2)$) varies from –33° to +20°C (Table III). Homogenization is always into liquid state by vapour disappearance. Type III & IV are biphase aqueous-carbonic inclusions at room temperature. This system involves two different critical points water (Critial Point 371°C) and CO_2 (31.1°C). The Rajpura-Dariba mineralization shows very reasonable CO_2-H_2O inclusions. At room temperature, these inclusions are immiscible, at high temperature the solubility increases dramatically. Kerrick and Jacobs (1981) developed Redlich-Kwong equation for homogeneous mixtures of CO_2-H_2O. During microthermometric analysis whenever temperature decreases, the freezing of CO_2-H_2O Fluid inclusions to a solid phase occur below -95 °C. During heating runs, melting of the carbonic phase (Tm CO_2) occurs either at the CO_2 triple point of -56.6 °C or over a small interval with depressed melting temperatures between -57.8 to -55.6 °C (Table II).

These measurements indicate that the carbonic phase in these inclusions is nearly pure CO_2, in contrast the inclusions with depressed melting temperatures that probably contain minor amounts of additional gas species, most likely CH_4 or N_2 (Roedder, 1984) Upon heating runs, more than one-half of the studied inclusions decrepitated prior to final homogenization, at temperatures from 215-290 °C. The homogenization of CO_2 in most inclusions is into the liquid phase by vapour disappearance ($LCO_2 + V \rightarrow LCO_2$). Only in a few inclusions the homogenization of CO_2 phases into vapour phase ($LCO_2 + V \rightarrow V$) was observed. The homogenization temperatures of CO_2 phases ($Th(CO_2)$) vary widely, with values ranging between +8° to +28°C (Table III). Temperature of total homogenization (Th(total)) also varies widely. In all the cases where measurements were possible, values of Th(total) was observed between 250°C to 290°C **(**Table III**)**.

The isochores are representing individual fluid inclusions studies and are widely distributed from 95°C to 290°C of temperature of homogenisation (average 192.50°C). The co-existing aqueous and carbonic inclusions were also studied and the plot shows intersecting isochores. Three populations of isochores observed between 95°C - 135°C, 200°C - 240°C and 250°C - 290°C. This may be interpreted in two ways viz (i) the parent fluid was originated from deeper depth with above 600 to 1100 bar pressure at 175 to 350°C temperature which come up to ground level and cooled down (ii) there may be two types of parental fluid, one originated from 2500 m depth with above 650 bar pressure at 340°C temperature and the other fluid originated from 1100 m depth with above 370 bar pressure at different temperature, which is almost similar with the suggested observation by Ameta and Sharma (2008). Some inclusions having variable degree of vapour and liquid phase at nearly the same temperature which indicate that possibly boiling of fluid took place, which suggest that, the depth of mineralization was 0-1800 m (Shepherd et al. 1985).

In view of the petrography of fluid inclusions, the aqueous biphase fluid inclusions show no daughter crystals and the observed data i.e. salinity of the inclusions are in favor of the observations made by Bodnar and Vityk, (1994). The calculated salinity of fluid, absence of daughter crystal, low gas content,

and the plot between salinity v/s homogenization temperatures suggests that the inclusions in the quartz veins are of epithermal in nature (Fig. 10). The epithermal formation of the fluid inclusions also suggest the low trapping pressures and therefore, the temperature of formation of quartz veins can be calculated from the range of homogenization temperatures of inclusions which are the histogram mean of homogenization temperatures (Wilkinson, 2001; Tun et al., 2014). The most characteristic feature noticed is the clustering in the diagram pointing some parameters which as follows. The trends of inclusion plots indicate the following possibilities (Shepherd et al. 1985).

1. Mixing with cooler, less saline fluid
2. Simple cooling
3. Boiling with slight cooling

The trend line of temperature of homogenization vs. salinity plot is shown in (Fig. 10) which indicates the mixing of fluids with moderate to high salinity at moderate temperature. The possibility for the contrasting fluid composition of type II and type III inclusions is fluid mixing of two different compositions. One composition is the moderate salinity fluid and other is CO_2 rich fluid. The type I inclusions are moderate to low salinity and low temperature indicating that the final stage of hydrothermal system at Rajpura-Dariba mineralization Belt might be involved of meteoric fluid.

CONCLUSION

The formation of Paleoproterozoic Carbonate-hosted Pb-Zn deposit in the Rajpura-Dariba Bethumni Belt, Rajasthan, India, has been investigated by detailed fieldwork and analyses of fluid inclusions by microthermometry. The hydrothermal system is characterized by the incursion of aqueous inclusion (Type I) into a pre-existing, low to medium salinity (4.15 to 13.26 Wt % NaCl eq.), low density (0.65to .92 g/cc) aqueous-carbonic fluid inclusion (Type III), and the progressive mixing of these two fluids. This mixture evolved towards lower to lower salinity, interpreted to monitor progressive dilution of the saline (Type I) by the pre-existing CO_2-dominated fluid (II). The epithermal formation of fluid inclusion also reveal, low internal pressure and got entrapped in absence of boiling condition and favored density driven mechanism.

The intersection of the isochors assign a fluid pressure and temperature of trapping at between 1.2 and 2 kbar, and 95°C to 290°C. The large temperature range of mineralization, points to the rapid cooling of a hot hydrothermal fluid injected into a cold host rock succession. The low temperature of aqueous fluid inclusion may provide evidence for mixing of magmatic fluid with meteoric waters.

ACKNOWLEDGMENT

The authors are thankful to Prof. R. Krishnamurthy Indian Institute Technology Roorkee (U.K.) for laboratory support in carrying out the investigation and Mr. Ajit Kumar Sahoo from the same department for fruitful scientific discussion and support and Chairman of Department of Geology, AMU Aligarh for providing necessary research facilities.

REFERENCES

Alam, J. (2019). Ore petrography and fluid inclusions studies of Pb and Zn deposits, Udaipur, Rajasthan, India. Unpublished Ph.D. thesis, Geology Department, Aligarh Muslim University, Aligarh. 199p

Ameta, S. S. & Sharma B. B. (2008). Geology, Metallogeny and Exploration of Concealed Lead-Zinc Deposit in Sindesar Khurd-Lathiyakheri Area, Rajsamand District, Rajasthan: Journal of the Geological Society of India, 72(3), 381-399.

Archer, D. G. (1992). Thermodynamic properties of the NaCl +H2O system: II. Thermodynamic properties of NaCl(aq), NaCl 2H2O(cr), and phase equilibria, Jour. Phys. Chem. Ref. Data, 28, 1–17.

Aulstead, K. L., Spencer, R. J., & Krouse, H. R., (1988). Fluid inclusion and isotopic evidence on dolomitization, Devonian of Western Canada: Geochimica et Cosmochimica Acta, 52, 1027-1035.

Basu, K. K. (1966). Systematic geological mapping in Bhilwara district Rajasthan'. Rep. - (Unpublished Geol, Surv. Ind. (F.S. 1965-66).

Bodnar, R. J., Lecumberri-Sanchez P., Moncada D. & Steele-MacInnis M. (2014). Fluid Inclusions in Hydrothermal Ore Deposits. In: Holland H.D. and Turekian K.K. (eds.) Treatise on Geochemistry, Second Edition, 13, 119-142. Oxford: Elsevier.

Bodnar, R. J, & Vityk M. O. (1994). Interpretation of microthermometric data for NaCl−H_2O fluid inclusions. In: De Vivo B, Frezzotti ML (eds) Fluid inclusions in minerals: methods and applications. Virginia Polytechnic Inst State Univ. Blacksburg, VA, 117–131.

Bodnar, R. J. (1993). Revised equation and table for determining the freezing point depression of H_2O-Nacl solutions. Geochimica et Cosmochimica Acta, 57(3), 683–684.

Coniglio, M., Sherlock, R., Williams-Jones, A.E., Middleton, D., and Frape, S.K., 1994, Burial and hydrothermal diagenesis of Ordovician car-bonates from the Michigan Basin, Ontario, Canada, in Purser, B., Tucker, M. and Zenger, D., eds., A volume in honor of Dolomieu: International Association of Sedimentologists, Special Publication 21, p. 231-254.

Conliffe, J., Wilton, D. H. C., Blamey, N. J. F. & Archibald, S. M. (2013) Paleoproterozoic Mississippi Valley Type Pb–Zn mineralization in the Ramah Group, Northern Labrador: Stable isotope, fluid inclusion and quantitative fluid inclusion gas analyses. Chemical Geol., 362, 211-223.

Diamond, L. W. (2001). Review of systematic CO_2-H_2O fluid inclusions. Lit hos 55, 69-99.

Diamond, L. W. (1994). Introduction to phase relations of CO2-H2O fluid inclusions, in Benedetto, De Vivo, and Maria, L.F., eds., Fluid inclusions in minerals: Methods and applications: Blacksburg, VA, Virginia Polytechnic Institute and State University, 131–158.

Gandhi, S. M. (2003). Rampura-Agucha zinc-lead deposit. Mem. Geol. Soc. India, no.55, 154.

Geological Survey of India. (1995). Geological Map of Rajpura-Dariba-Bethumni-Surawas Belt. Records Of GSI, 129 (7),1995.

Gupta , B. C. (1934). The Geology of Central Mewar, Mem. Geo. Surv. Ind. V. 65, Pt 2nd, 107-168.

Gupta, S. N, Arora, Y. K., Mathur R. K., Iqbuluddin, Prasad B., Sahai, T. N. & Sharma, S. B. (1980). Lithostratigraphic map of Aravalli region, southern Rajasthan and northern Gujarat; Geol. Surv. India.

Haynes, F. M., Beane, R. E. & Kesler, S. E. (1989). Simultaneous transport of metal and reduced sulfur, Mascot-Jefferson City zinc district, East Tennessee; evidence from fluid inclusions. Amer. Jour. Sci., 289(8), 994-1038.

Heron, A. M., (1953). Geology of Central Rajasthan, Mem.79, Geol. Survey of India, 339.

Huizenga, J. M., Gutzmer, J., Banks, D. & Greyling, L. (2006). The Paleoproterozoic carbonate-hosted Pering Zn–Pb deposit, South Africa. II: fluid inclusion, fluid chemistry and stable isotope constraints. Mineralium Deposita, 40(6-7), 686.

Jones, H. D. & Kesler, S. E. (1992). Fluid inclusion gas chemistry in east Tennessee Mississippi Valley-type districts: evidence for immiscibility and implications for depositional mechanisms. Geochim. Cosmochim. Acta, 56(1), 137-154.

Kerrick, D. M. & Jacobs, G. K. (1981). A modified Redlich-Kwong equation for H_2O, CO_2, and H_2O-CO_2 mixtures. Amer. J. Sci. 281, 735-767.

Kesler, S. E., Reich, M., & Jean, M. (2007). Geochemistry of fluid inclusion brines from Earth's oldest Mississippi Valley-type (MVT) deposits, Transvaal Supergroup, South Africa. Chemical Geol., 237, 274-288.

Morrow, D., (1998). Regional subsurface dolomitization, Models and con-straints: Geoscience Canada, 25 (2), 57-70.

Nelson, J., Paradis, S., Christensen, J., & Gabites, J. (2000). Canadian Cordilleran Mississippi Valley-type deposits: A case for Devonian- Mississippian back-arc hydrothermal origin: Economic Geology, 97, 1013-1036.

Poddar, B. C. & Chatterjee, A. K.. (1965). Report on investigation of Dariba-Rajpura-Bathumni mineralised zone, Udaipur district Rajasthan (Unpublished report) Geol. Surv. India F-S (1964-65)

Raja Rao, C. S. (1967). On the age of Precambrian Group of Rajasthan. J. Mm. Met. and Fuel. 15(9).

Roedder, E. (1984). Fluid inclusions. Mineralogical Society of America, Reviews in Mineralogy, 12, Ed. Ribbe, P. H. 646.

Roy, A. B. & Das, A. R. (1985). A study of time relation between movements, metamorphism and granite emplacement in the middle-Proterozoic Delhi Supergroup of Rajasthan. J Geol. Soc India 26: 726-733.

Roy, A. B. (1988). Stratigraphic and tectonic framework of the Aravalli Mountain Range In Precambrian of the Aravalli Mountain, Rajasthan, India (ed. A. B. Roy) Memoir, Geological Society of India No. 7, 3-31.

Samaddar, U. & Das Gupta S. (1990). Investigation for basemetal in North Sidesar Ridge block, Dariba-Bethunmi belt, Udaipur district, Rajasthan. Rec. Geol. Surv. Ind, 123, 7, 72-75.

Sharma, B. L., Chauhan, N. K. & BHU, H., (1988). Strtictural geometry and deformation history of the early Proterozoic Aravalli rocks of Bagdunda, district Udaipur, Rajasthan. Mem. Geol. Soc. India, 7, 169-191.

Sharma, K. K & Rahman, A. (1995). Occurrence and petrogenesis of Loda Pahar trondhjemitic gneiss from Bundelkhand craton, central India: Remnant of early crust. Curr. Sci. 69, pp. 613-616.

Shepherd T.J., Rankin, A. H. & Alderton, D. H. M. (1985). A Practical Guide to Fluid inclusion studies, Glasgow (Blackie) and New York (Chapman and Hall), 239.

Tun, M. M., Warmada, I. W., Idrus, A., Harijoko, A., Verdiansyah, O. & Watanabe, K. (2014). Fluid inclusion studies of the epithermal quartz veins from Sualan prospect, west Java, Indonesia, Jour. SE Asian Appld. Geol., 6(2), 62–67.

Van den Kerkhof, A. M., & Hein, U. F. (2001). Fluid inclusion petrography. Lithos 55, 27-47

Wilkinson, J.J. (2001). Fluid Inclusions in Hydrothermal Ore Deposits. Lithos, 55, 229-272. http://dx.doi.org/10.1016/S0024-4937(00)00047-5.

Yadav, P. K. & Sharma, B.B. (1991). A report on the exploration for leadzinc ores in the North Sindesar Ridge (South) South Extension and Central blocks, Dariba-Bethunmi belt, Udaipur district, Rajasthan. Unpub. GSI report for F.S.1989-90.

***